

Energies and radial distributions of B_s mesons on the lattice

(UKQCD Collaboration)

J. Koponen^{1,*}

¹*Department of Physical Sciences and Helsinki Institute of Physics,
P.O. Box 64, FIN-00014 University of Helsinki, Finland*

This is a follow-up to our earlier work for the energies and the charge (vector) and matter (scalar) distributions for S-wave states in a heavy-light meson, where the heavy quark is static and the light quark has a mass about that of the strange quark. We now study excited states of these mesons with higher angular momentum and with radial nodes.

The calculation is carried out with dynamical fermions on a $16^3 \times 32$ lattice with a lattice spacing $a \approx 0.10$ fm. The lattice configurations were generated by the UKQCD Collaboration. Attempts are now being made to understand these results in terms of the Dirac equation. In nature the closest equivalent of this heavy-light system is the B_s meson, which allows us to compare our lattice calculations to experimental results (where available) or give a prediction where the P-wave states should lie. We pay particular attention to the spin-orbit splitting, to see which one of the states (for a given angular momentum L) has the lower energy.

I. MOTIVATION

There are several advantages in studying a heavy-light system on a lattice. Our meson is much more simple than in true QCD: one of the quarks is static with the light quark “orbiting” it. This makes it very beneficial for modelling. On the lattice an abundance of data can be produced, and we know which state we are measuring – the physical states can be a mixture of two or more configurations, but on the lattice this complication is avoided. However, our results on the heavy-light system can still be compared to the B_s meson experimental results.

II. MEASUREMENTS AND LATTICE PARAMETERS

We have measured both angular and radial excitations of heavy-light mesons, and not just their energies but also some radial distributions. Since the heavy quark spin decouples from the game we may label the states as $L_{\pm} = L \pm \frac{1}{2}$, where L is the angular momentum and $\pm \frac{1}{2}$ is the spin of the light quark.

The measurements were done on a $16^3 \times 32$ lattice. We have two degenerate quark flavours with a mass that is close to the strange quark mass. The lattice configurations were generated by the UKQCD Collaboration. More details of the different lattices used in this study can be found in Refs. [1], and references therein. Two different levels of fuzzing (2 and 8 iterations of conventional fuzzing) were used in the spatial directions to permit the extraction of the excited states.

III. 2-POINT CORRELATION FUNCTION

The 2-point correlation function (see Figure 1) is defined as

$$C_2(T) = \langle P_t \Gamma G_q(\mathbf{x}, t+T, t) P_{t+T} \Gamma^\dagger U^Q(\mathbf{x}, t, t+T) \rangle, \quad (1)$$

where $U^Q(\mathbf{x}, t, t+T)$ is the heavy (infinite mass)-quark propagator and $G_q(\mathbf{x}, t+T, t)$ the light anti-quark propagator. P_t is a linear combination of products of gauge links at time t along paths P and Γ defines the spin structure of the operator. The $\langle \dots \rangle$ means the average over the whole lattice. The energies (m_i) and amplitudes (a_i) are extracted by fitting the C_2 with a sum of exponentials,

$$C_2(T) \approx \sum_{i=1}^{N_{\max}} a_i e^{-m_i T}, \text{ where } N_{\max} = 2 - 4, T \leq 14. \quad (2)$$

*Electronic address: jonna.koponen@helsinki.fi

nL±-1S	Lattice 1	Lattice 2	Lattice 3	nL±-1S	Lattice 1	Lattice 2	Lattice 3
1S	0	0	0	2S	0.65(2)	0.820(15)	0.78(3)
1P-	0.44(4)	0.40(2)	0.41(3)	2P-	1.34(6)	1.32(2)	1.30(5)
1P+	0.59(4)	0.47(3)	0.40(4)	2P+	1.53(5)	1.38(3)	1.30(6)
1D±	-	0.96(3)	0.98(6)	2D±	-	1.47(2)	1.60(5)
1D-	0.89(5)	0.83(3)	0.82(5)	2D-	1.75(4)	1.694(15)	1.71(4)
1D+	0.92(7)	0.87(3)	0.92(3)	2D+	1.72(6)	1.73(2)	1.77(2)
1F±	1.30(5)	1.19(4)	1.15(3)	2F±	2.01(2)	1.941(15)	1.939(12)

TABLE I: Heavy-light meson energy differences in GeV. Lattice 1 uses a static heavy quark, whereas Lattices 2 and 3 are slightly smeared in the time direction. Lattice 2 uses APE type smearing and Lattice 3 uses hypercubic blocking. See [2] for details.

Fuzzing indices have been omitted for clarity.

IV. ENERGY SPECTRUM AND SPIN-ORBIT SPLITTINGS

The energy spectrum obtained is shown in Fig. 2 and in Table I. There seems to be some spread in the extracted energy for the P+ state between the different lattices, but the reason for this is not understood yet. The energy of the D+- state was expected to be near the spin average of the D- and D+ energies, but it turned out to be a poor estimate of this average. Thus it is not clear whether or not the F+- energy is near the spin average of the two F-wave states, as was hoped. Our earlier results can be found in Ref. [1].

One interesting point to note here is that the spin-orbit splitting of the P-wave states is small, almost zero. We extracted the energy difference of the P+ and P- states in two different ways:

1. *Indirectly* by simply calculating the difference using the energies given by the fits in Eq. 2, when the P+ and P- data are fitted separately.
2. Combining the P+ and P- data and fitting the ratio $\frac{C_2(P+)}{C_2(P-)}$, which enables us to go *directly* for the spin-orbit splitting, $m_{P+} - m_{P-}$.

The results of the fits are (-5 ± 45) MeV and (11 ± 13) MeV, respectively. D-wave spin-orbit splitting was also extracted in a similar manner, giving the results (102 ± 54) MeV and (124 ± 18) MeV, respectively.

To obtain predictions of the B_s meson excited state energies, we can now interpolate between the static heavy quark lattice calculations and D_s meson experimental results, i.e. interpolate between the static quark and the charm quark. Linear extrapolation seems to work well, as can be seen in Fig. 3. The P-wave states seem to lie near the BK thresholds.

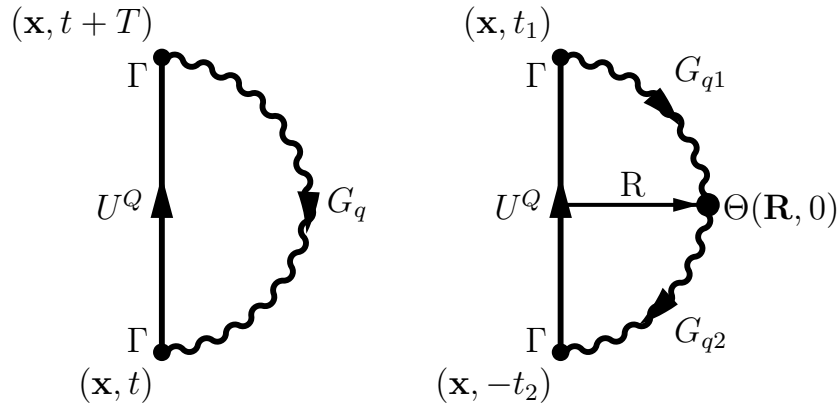


FIG. 1: On the left: Two-point correlation function. On the right: Three-point correlation function.

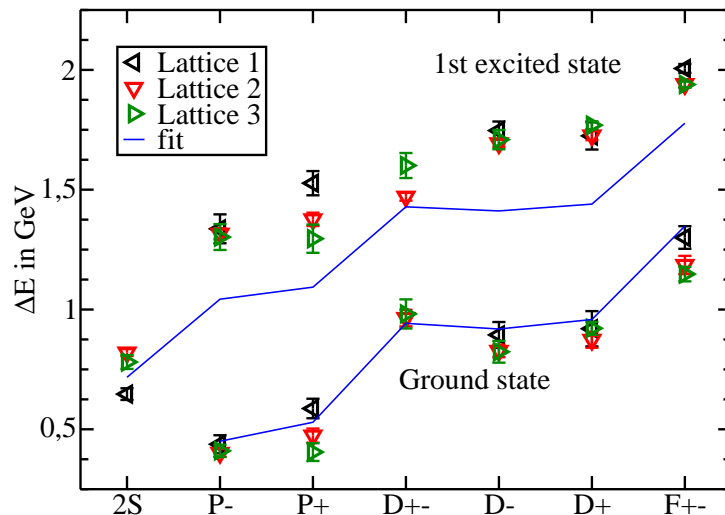


FIG. 2: Energy spectrum of the heavy-light meson. Here $L+(-)$ means that the light quark spin couples to angular momentum L giving the total $j = L \pm 1/2$. $2S$ is the first radially excited $L = 0$ state. The $D+-$ is a mixture of the $D-$ and $D+$ states, and likewise for the $F+-$. Energies are given with respect to the S -wave ground state ($1S$). Here $a = 0.115(3)$ fm was used to convert the energies to physical units. The error bars shown here contain statistical errors from the lattice calculations and the uncertainty in the extracted lattice spacing. The solid line on the one-body Dirac equation – see section VI for details.

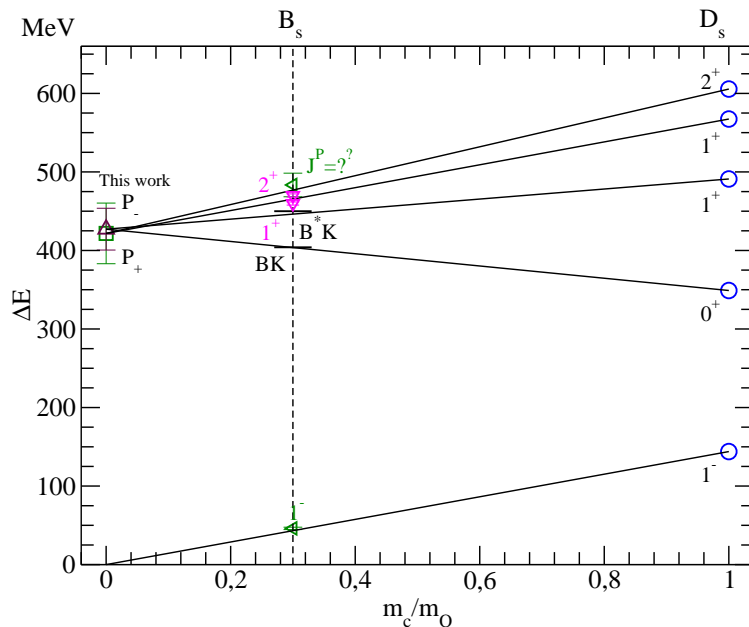


FIG. 3: Interpolation to the b -quark mass. The experimental data is from [3]. For another lattice group's $m_c/m_Q = 0$ results see [4].

V. RADIAL DISTRIBUTIONS: 3-POINT CORRELATION FUNCTION

For evaluating the radial distributions of the light quark a 3-point correlation function shown in Fig. 1 is needed. It is defined as

$$C_3(R, T) = \langle \Gamma^\dagger U^Q \Gamma G_{q1} \Theta G_{q2} \rangle. \quad (3)$$

This is rather similar to the 2-point correlation function in Eq. 1. We have now two light quark propagators, G_{q1} and G_{q2} , and a probe $\Theta(R)$ at distance R from the static quark (γ_4 for the vector (charge) and 1 for the scalar (matter) distribution).

Knowing the energies m_i and the amplitudes a_i from the earlier C_2 fit, the radial distributions, $x^{ij}(R)$'s, are then extracted by fitting the C_3 with

$$C_3(R, T) \approx \sum_{i,j=1}^{N_{\max}} a_i e^{-m_i t_1} x^{ij}(R) e^{-m_j t_2} a_j. \quad (4)$$

The results are plotted in Figs. 4 and 5. The error bars in these figures show statistical errors only. See [5] and [2] for earlier calculations.

VI. A MODEL BASED ON THE DIRAC EQUATION

A simple model based on the Dirac equation is used to try to describe the lattice data. Since the mass of the heavy quark is infinite we have essentially a one-body problem. The potential in the Dirac equation has a linearly rising scalar part, $b_{\text{sc}}R$, as well as a vector part $b_{\text{vec}}R$. The one gluon exchange potential, $a_{\text{OGE}} \cdot V_{\text{OGE}}$, is modified to

$$V_{\text{OGE}}(R) \propto \int_0^\infty dk j_0(kR) \ln^{-1} \frac{k^2 + 4m_g^2}{\Lambda_{\text{QCD}}^2}, \quad (5)$$

where $\Lambda_{\text{QCD}} = 260$ MeV and the dynamical gluon mass $m_g = 290$ MeV (see [6] for details). The potential also has a scalar term $m\omega L(L+1)$, which is needed to increase the energy of higher angular momentum states. However, this is only a small contribution (about 30 MeV for the F-wave).

The solid lines in the radial distribution plots are predictions from the Dirac model fit with $m = 0.088$ GeV, $a_{\text{OGE}} = 0.81$, $b_{\text{sc}} = 1.14$ GeV/fm, $b_{\text{vec}} \approx b_{\text{sc}}$ and $\omega = 0.028$. These are treated as free parameters with the values obtained by fitting the ground state energies of P-, D- and F-wave states and the energy of the first radially excited S-wave state (2S). Note that the excited state energies in Fig. 2 were not fitted.

VII. CONCLUSIONS

- There is an abundance of lattice data, energies and radial distributions, available for this B_s -like system.
- The P-wave spin-orbit splitting is small (essentially zero), which supports the symmetry $b_{\text{vec}} = b_{\text{sc}}$ as proposed in [7]. The D-wave spin-orbit splitting is clearly non-zero and positive, whereas another lattice group seems to find it to be slightly negative (see [4]).
- The energies and radial distributions of S-, P- and D-wave states can be qualitatively understood by using a one-body Dirac equation.

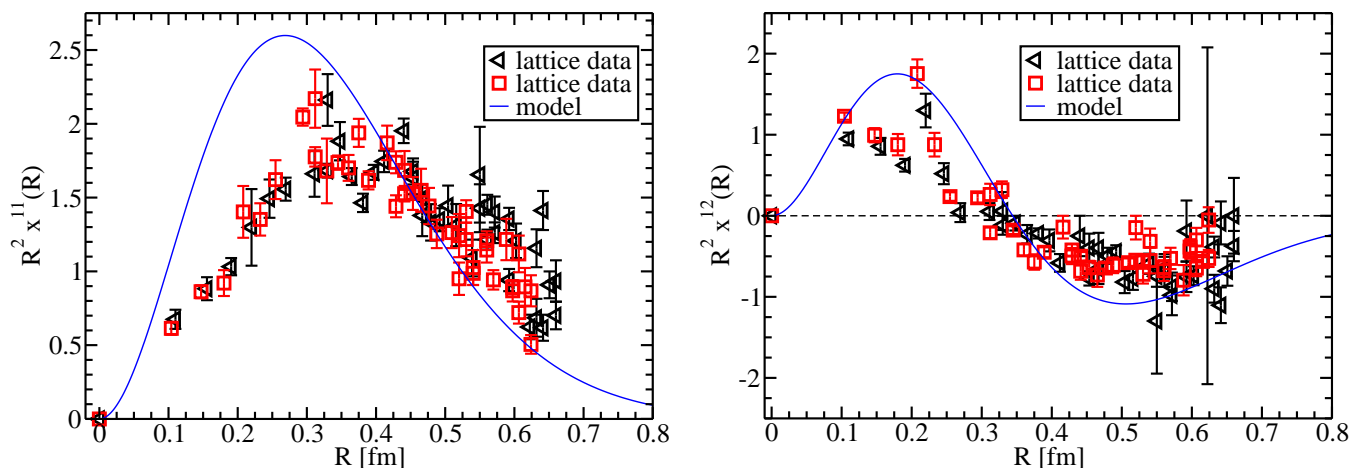


FIG. 4: On the left: The S-wave ground state charge distribution. The label “model” on the solid line refers to the model presented in section VI. On the right: The S-wave ground state and 1st excited state charge distribution overlap. Note that we see one node, as expected from the Dirac equation.

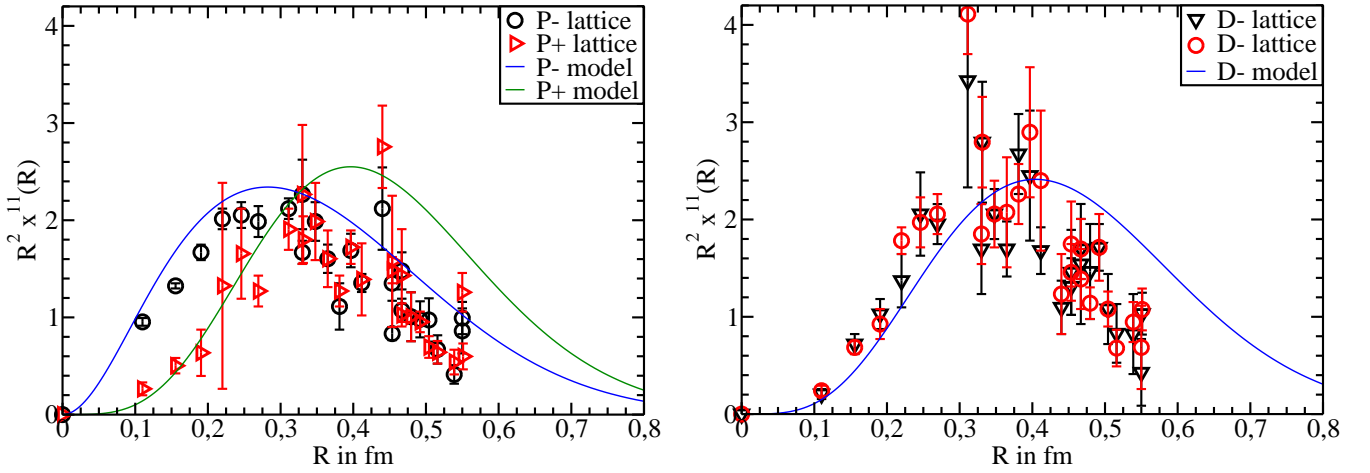


FIG. 5: On the left: The P-wave ground state charge distributions. The P+ distribution has a peak a bit further out than the P−, which is expected. The solid lines are predictions from the model in section VI. On the right: The D− ground state charge distribution.

Acknowledgements

I am grateful to my supervisor A. M. Green and to our collaborator, Professor C. Michael. I wish to thank the UKQCD Collaboration for providing the lattice configurations. I also wish to thank the Center for Scientific Computing in Espoo, Finland, for making available the computer resources. The EU grant HPRN-CT-2002-00311 Euridice is also gratefully acknowledged.

-
- [1] UKQCD Collaboration, A. M. Green, J. Koponen, C. Michael, C. McNeile and G. Thompson, Phys. Rev. D 69, 094505 (2004); UKQCD Collaboration, J. Koponen, [hep-lat/0411015](#)
 - [2] UKQCD Collaboration, J. Koponen, PoS LAT2006 (2006) 112
 - [3] W.-M. Yao *et al.*, J. Phys. G 33, 1 (2006); CDF and DØ collaborations, R. K. Mommensen, [hep-ex/0612003](#)
 - [4] J. Foley, A. Ó Cais, M. Peardon and S. Ryan, PoS LAT2006 (2006) 196
 - [5] UKQCD Collaboration, A. M. Green, J. Koponen, C. Michael and P. Pennanen, Phys. Rev. D 65, 014512 (2002) and Eur. Phys. J. C 28, 79 (2003); UKQCD Collaboration, A. M. Green, J. Ignatius, M. Jahma, J. Koponen, C. McNeile and C. Michael, PoS LAT2005 (2005) 205
 - [6] T. A. Lähde, C. Nyfält and D. O. Riska, Nucl. Phys. A674, 141 (2000)
 - [7] P. R. Page, T. Goldman and J. N. Ginocchio, Phys. Rev. Lett. 86, 204 (2001)